

## Design and Analysis of Properties MASnI<sub>3</sub> Nanostructures Doped with Cu<sub>2</sub>O

Ankit Mishra<sup>1</sup>, Manoj Kumar Nigam<sup>2,\*</sup>

<sup>1</sup> Department of Electrical Engineering, MATS University, Raipur, India

<sup>2</sup> Department of Electrical Engineering, MATS University, Raipur, India

(Received 15 June 2023; revised manuscript received 22 August 2023; published online 30 August 2023)

In the paper, we simulate methylammonium tin iodide MASnI<sub>3</sub> with Zinc Oxide-Aluminum nZnO-Al doped with Cu<sub>2</sub>O. This base structure shows promising results in comparison to previous data. We use SCAPS-1D high simulation tool to investigate the *I-V*, admittance, band gap and current density of the base structure FTO/Cu<sub>2</sub>O/MASnI<sub>3</sub>/nZnO-Al. Positive results and a PCE of 24.2 % were attained in this study. Here, an anode composition with such a high work potential is needed for the device to operate more effectively. A novel lead-free perovskite-based photovoltaic array based upon MASnI<sub>3</sub> solar cell with varied parameters (SCAPS-1D) was built and modelled using the one-dimensional photovoltaic solar capacitance simulation. The results showed that the thickness of the absorber layer could have a significant impact on the device's PCE, and it was determined that 250 nm was the ideal thickness for the absorber layer. In these studies, we introduced two different defect density at each PEC layer to create a standard environment and the results are promising. Utilizing different conducting materials and layers, including electrode, ETL, and HTL layers, the effect on the ways is studied. At a temperature of 300 K, the PEC performs admirably. It is also observed that a shift in temperature might reduce the device's overall effectiveness.

**Keywords:** MASnI<sub>3</sub>, nZnO-Al, Nanostructures, Perovskite, SCAPS-1D, Computational Modeling

DOI: [10.21272/jnep.15\(4\).04020](https://doi.org/10.21272/jnep.15(4).04020)

PACS numbers: 07.10.Cm, 68.35.Iv

### 1. INTRODUCTION

The perovskite solar cell (PSC) has emerged as one of the most promising photovoltaic technologies, with a power conversion efficiency (PCE) of more than 25 % in a single junction design. This technology can compete with the conventional silicon solar cell and is rapidly moving towards commercialization [1]. However, a few key challenges, such as the device's stability in the air under light and the toxicity of the chemicals used, are hampering PSC's commercialization advancement. The ABX<sub>3</sub> perovskite structure with methylammonium (CH<sub>3</sub>NH<sub>3</sub><sup>+</sup>), formamidinium (NH<sub>2</sub>CHNH<sub>2</sub><sup>+</sup>), and cesium (Cs<sup>+</sup>) in the A cation site lead (Pb) in the B cation site, and iodine (I) and bromine (Br) in the X anion site has shown to be the most successful in perovskite solar cells so far. The main environmental worry with perovskite solar cells, however, is the presence of toxic and heavy elements like lead throughout their whole existence. Because of this, in addition to having great efficiency, research groups and business leaders are less optimistic about its future, which opens the door for lead-free perovskite materials [2]. Wideband gaps in many lead-free perovskite absorber materials make them viable replacements for harmful lead-containing perovskites. Direct bandgap methylammonium tin iodide is one example.

MXene is a family of transition metal carbides and nitrides that exist in two dimensions (2D). They have the generic formula M<sub>x</sub>Ti<sub>y</sub>, where M stands for transition metal and *x* and *y* stand for the amount of metal and

nonmetal atoms in the compound, respectively. Due to their distinctive qualities, such as excellent electrical conductivity, mechanical strength, and chemical stability, these materials have garnered a lot of interest in recent years. The first MXene materials were created in 2011 by a group of scientists at Drexel University under the direction of Yury Gogotsi. The researchers found that a new class of 2D materials may be produced by selectively etching the A-groups (such as Al, Ga, or In) from MAX phases (such as Ti<sub>3</sub>AlC<sub>2</sub>) [3, 4].

Even though tin-based perovskite solar cells have seen significant progress in the laboratory, additional advancement is still conceivable by optimizing various parameters and device configurations that can serve as a roadmap for future experimental advancement. Methylammonium tin iodide (MASnI<sub>3</sub>) based perovskite has been investigated, examined, and researched with various parameters through this simulation effort [5, 6]. A 1D-solar cell capacitance simulator is used in this study to simulate the efficiency of the device under AM1.5G light (SCAPS, ver. 3.3.07). Variables such as the thickness and doping levels of different layers, such as the electron transport layer, the perovskite absorber layer, and the hole transport layer, have been modified and their impacts have been considered for future performance improvement. Additionally, the defect densities have been considered. Different HTLs and their effects have been studied, and eventually, an optimum configuration has been developed to offer the highest efficiency of 24.43 %. This configuration was produced using a variety of

\* [drmanojk@matsuniversity.ac.in](mailto:drmanojk@matsuniversity.ac.in)

The results were presented at the 3<sup>rd</sup> International Conference on Innovative Research in Renewable Energy Technologies (IRRET-2023)

analysis techniques and theoretical modeling [7, 8].

These cells' performance may be optimized using a variety of techniques, such as:

1) Materials optimization – choosing the ideal mix of materials and their characteristics may greatly improve the cell's overall performance.

2) Structural optimization – The efficiency of the cell may be increased by precisely adjusting the shape and dimension of the MASnI<sub>3</sub> nanostructures.

3) Electron transport optimization – Controlling the distribution of flaws and impurities in the materials allows for the optimization of electron transport across the cell.

4) Light harvesting improvement – by enhancing the active layer's thickness and the materials' optical characteristics, the cell's capacity to absorb light may be boosted.

## 2. DEVICE SIMULATION

With the goal of determining the optical and electrical characteristics most suited for obtaining high power conversion efficiency, the simulation was run using the SCAPS-1D program. The Electronics and Information Systems (ELIS) Department at the University of Ghent in Belgium is where SCAPS software is created. Poisson's equation and the continuity equation of both charge carriers are used by SCAPS-1D to operate. Up to 7 layers may be changed to configure the various types of solar cells, and simulations can be run in both dimly-lit and well-lit environments. The following equations can be entered into the program to calculate output results: The semiconductor Poisson's equation is given by equation (2) [9].

Because of their opposing effective charges, electrons, and holes are predicted to attract one other when they are sufficiently close. When the thermal energy is low enough, the coulomb attraction causes electrons and holes to circle each other around their common center of mass. Because it is the initial excited state of the one-electron energy band, this bound electron-hole pair is referred to as an exciton [10]. The coulomb attraction reduces the energy of an electron that would otherwise be in the conduction band, resulting in a succession of permissible energy levels in the forbidden bandgap immediately below the conduction band.

$$R_{n,p} = \frac{qn_p}{\epsilon\epsilon_0} (\mu_n(E) + \mu_p(E)), \quad (1)$$

$$J = qv_n\mu_n\varepsilon + qv_p\mu_p\varepsilon, \quad (2)$$

The potential in the model electrodes is calculated using Poisson's equation. Investigating performance, efficiency, and ways to enhance them is beneficial. The fundamental link between charge and an electric field is provided by this equation [11,12].

$$\text{div}(\epsilon\nabla\phi) = -\rho, \quad (3)$$

The standard drift and diffusion components are included in the heterostructure continuity equation,

nevertheless, the drift current contains the changes in electron affinity, and the classical electric field and a quasi-electric field exist. Similarly, in addition to the classical diffusion current, another component of current develops as the density of states fluctuates spatially. The band parameters are included in the continuity equation to account for these effects [13]. The continuity equations are shown in equations (4, 5), where  $J_n$  represents electron current density,  $J_p$  represents hole current density, and  $R$  represents the rate of carrier recombination [14]. There are two general phenomena that conduct current flow in semiconductors. The influence of the electric field produces minority charge carrier drift, and the concentration gradient produces diffusion current. The continuity equations provide Drift-Diffusion Current Relations:

$$J_n = qv_n\mu_n\varepsilon + qD_n \frac{dn}{dx}, \quad (4)$$

$$J_p = qv_p\mu_p\varepsilon - qD_p \frac{dp}{dx}, \quad (5)$$

$$J_{cond} = J_n + J_p, \quad (6)$$

$$I_p v = I_p v - I_o \left[ e^{\left[ \frac{q(V_p v + R_s I_p v)}{n k T c} \right]} - 1 \right] - \frac{V_p v + R_s I_p v}{R_p}, \quad (7)$$

Carrier densities in PSC transport layers (TLs) are frequently several orders of magnitude greater than in the perovskite layer due to high effective doping levels and band offsets between the layers [15]. As a result, in these layers upon layer, the Boltzmann assumption cannot be ensured to be valid, and also the charge carrier model is adjusted to provide for a generic (potentially non-Boltzmann) predictive method. We assume that conduction electrons in the electron transport layer (ETL) are characterized by SE and valence holes in the hole transport layer (HTL) by SH. As a result, in order to account for the statistical model used, the equations for current densities in the transport layers must be modified.

Figure 1 shows the Solar PV structure FTO/Cu<sub>2</sub>O/MASnI<sub>3</sub>/nZnO-Al.

Currently, we do.

$$j^n = \mu_E k_B T n \frac{\partial}{\partial x} \left[ S_E^{-1} \left( \frac{n}{g_E^E} \right) - \frac{q\phi}{k_B T} \right], \quad (8)$$

in the ETL

$$j^p = -\mu_H k_B T p \frac{\partial}{\partial x} \left[ S_H^{-1} \left( \frac{p}{g_H^H} \right) + \frac{q\phi}{k_B T} \right], \quad (9)$$

In the HTL.

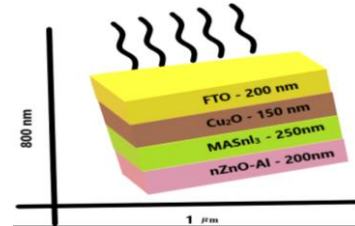


Fig. 1 – Solar PV structure FTO/Cu<sub>2</sub>O/MASnI<sub>3</sub>/nZnO-Al

Structure *n*ZnO-Al (Zinc Oxide-Aluminum) is a material that is used as a transparent conductor in the fabrication of solar cells. The material is attractive for this use because it has high electrical conductivity and is also transparent, allowing light to pass through to reach the photovoltaic material below.

This material is commonly used in thin film solar cells, where a layer of *n*ZnO-Al is deposited onto a substrate and serves as the front electrode. The combination of high conductivity and transparency make *n*ZnO-Al an important component in the production of efficient and cost-effective solar cells.

### 3. RESULTS AND DISCUSSIONS

Using tabular parameters compiled from numerous hypothetical and experimental works, SCAPS simulations were run. The performance of a perovskite solar cell is significantly influenced by each component. By constructing fictitious structures and analyzing studies of solar PV, we can test the device's performance using data from transport layers from previously published papers. It is possible to further implement the base structure FTO/Cu<sub>2</sub>O/MASnL<sub>3</sub>/*n*ZnO-Al to produce the fabricated sheet because it yields promising results. The variation aids in assessing the performance of the device model with various HTL, which turn out to be the decisive element in selecting the most suited material as HTL. In Fig. 2 shown the graph between admittance Vs Energy and Fig. 1 shows the parameters for simulation.

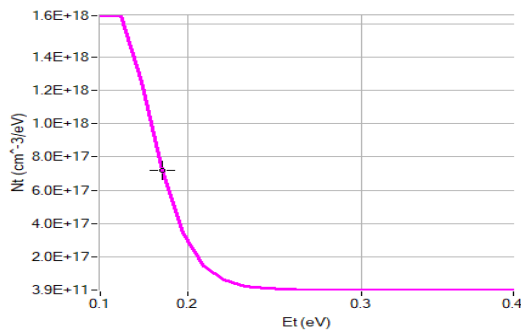


Fig. 2 – Shows the Admittance vs Energy

We have simulated the Solar PV structure FTO/Cu<sub>2</sub>O/MASnL<sub>3</sub>/*n*ZnO-Al in three condition that is AM1.5 solar illuminator, second in normal condition and thirdly in Sun condition. Fig. 3, 4 and 5 represents the graph between different parameters. In Fig. 6, we simulated the structure in two different perspectives i.e., one with the base structure FTO/Cu<sub>2</sub>O/MASnL<sub>3</sub>/*n*ZnO-Al. Secondly, we use AM 1.5 to boost the structure. While doing thing this efficiency is increases with 9 % to 24.2 %. In this paper we also simulate the previous work published by A.K. Singh et al. They simulate the structure with the base structure of Au/HTL/MASnL<sub>3</sub>/TiO<sub>2</sub>/FTO/Glass with the efficiency of 27 %. *n*ZnO-Al is a composite material made by combining zinc oxide (ZnO) and aluminum (Al). The combination of these two materials results in a material with unique

electrical, optical, and mechanical properties that can be utilized in a variety of applications. We used as a transparent conducting electrode in solar cells, where it provides high transparency and low resistivity. In figure (4), the overall structure band gap increases to 3.17 eV.

Table 1 – Parameters for Simulation

Material Property	Cu <sub>2</sub> O	FTO	MASnL <sub>3</sub>	<i>n</i> ZnO-Al
Thickness(nm)	150	200	250	200
Bandgap (eV)	2.17	3.2	1.3	1.2
Electron affinity (eV)	3.2	4.4	4.17	4.5
Dielectric Permittivity	7.5	9	6.5/10	10
CB effective density of states (cm <sup>-3</sup> )	2 × 10 <sup>18</sup>	2.2 × 10 <sup>18</sup>	1 × 10 <sup>18</sup>	1 × 10 <sup>18</sup>
VB effective density of states (cm <sup>-3</sup> )	1.81×10 <sup>19</sup>	1.81 × 10 <sup>19</sup>	1 × 10 <sup>19</sup>	1 × 10 <sup>19</sup>
Electron thermal velocity (cm/s)	1 × 10 <sup>7</sup>	1 × 10 <sup>7</sup>	1 × 10 <sup>7</sup>	1 × 10 <sup>7</sup>
Hole thermal velocity (cm/s)	1 × 10 <sup>7</sup>	1 × 10 <sup>7</sup>	1 × 10 <sup>7</sup>	1 × 10 <sup>7</sup>
Electron Mobility(cm <sup>2</sup> /V.s)	20	20	1.6	5
Hole Mobility(cm <sup>2</sup> /V.s)	80	10	1.6	5
1) Defect Density N <sub>t</sub> (cm <sup>-3</sup> )	2 × 10 <sup>15</sup>	1 × 10 <sup>19</sup>	2 × 10 <sup>15</sup>	2 × 10 <sup>15</sup>
2) Defect Density N <sub>t</sub> (cm <sup>-3</sup> )	1 × 10 <sup>14</sup>	1 × 10 <sup>15</sup>	4.5 × 10 <sup>16</sup>	4.5 × 10 <sup>16</sup>

Band Diagram

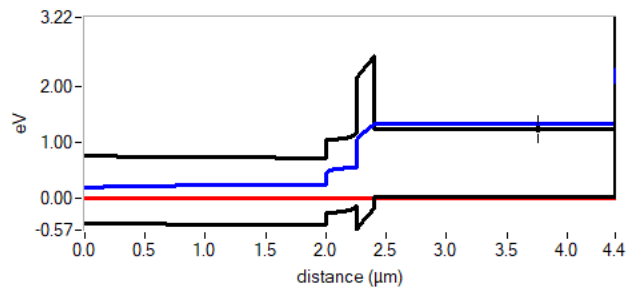


Fig. 3 – Energy Band Gap Vs Distance

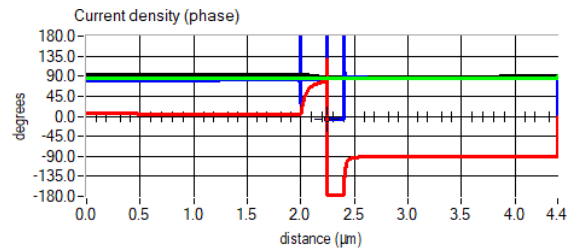


Fig. 4 – AC Current Density vs Distance

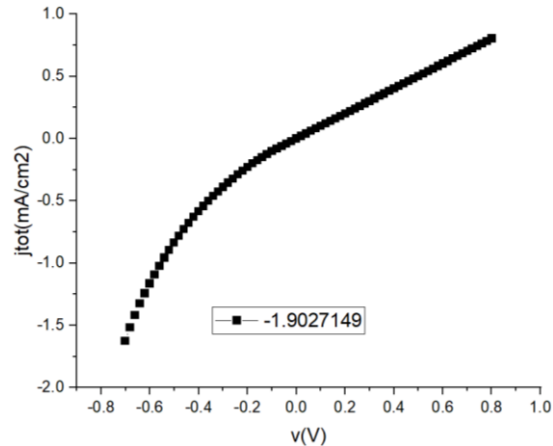


Fig. 5 – Current Density Total Vs Voltage

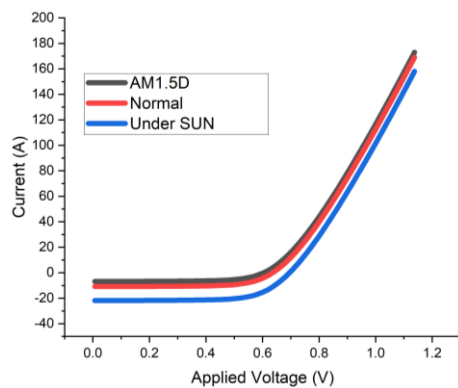


Fig. 6 – Current Density Vs Voltage

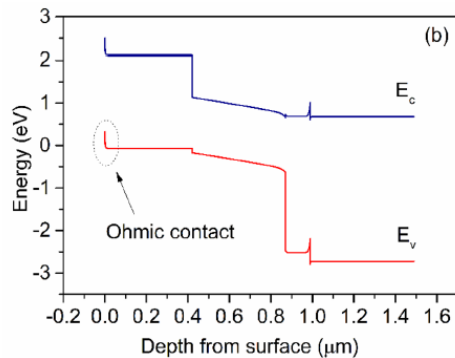


Fig. 6 – Band Diagram of PSC with ohmic contact.

Understanding photovoltaic performance at high temperatures is one of the key issues in figuring out how to stabilize photovoltaic efficiency. Due to layer deformation at high temperatures, the majority of solar cell architectures display performance instability. Recent studies have shown that it is possible to improve the performance stability of optoelectronic devices based on perovskites at high temperatures. The temperature range of the simulation study was changed from 300 K to 500 K in order to examine the impact of temperature on solar cell performance. As shown in Figure, In particular, the photovoltaic array's efficiency is significantly harmed by temperature changes (see Fig. 6). From 24.2 % at 300 K to 9.1 % at 500 K, the PEC dramatically drops as temperature rises. Temperature has a similar impact on solar cell performance, according to numerous studies. As the temperature rises, efficiency declines along with the charge transport diffusion layer. The displacement stress increases primarily on the layers as the temperature rises, leading to interfacial flaws and poor layer connectivity. The absorber layer's rate of adsorption increases as a result of the weak interconnectivity, which also causes the series resistance to rise and the transport properties to deteriorate. Solar cells' performance suffers as a result. But at an operational temperature of about 300 K, the model performs at its peak.

#### 4. CONCLUSION

A novel lead-free perovskite-based photovoltaic array based upon  $\text{MASnI}_3$  solar cell with varied parameters (SCAPS-1D) was built and modelled using the one-dimensional photovoltaic solar capacitance simulation. The results showed that the thickness of the absorber layer could have a significant impact on the device's PCE, and it was determined that 250 nm was the ideal thickness for the absorber layer. Utilizing different conducting materials and layers, including electrode, ETL, and HTL layers, the effect on the ways will be studied. At a conventional temperature of 300 Kelvin, the PEC performs admirably, with a conventional efficiency of 24 %. We also discovered that a shift in temperature might reduce the device's overall effectiveness. The charge transfer has an impact on the device's durability. While the doping concentration was increased to  $1.81 \times 10^{19}$ , the solar cell's performance remained constant. In these studies, we introduced two different defect density at each PEC layer to create a standard environment and the results are promising.

#### REFERENCES

1. K. Brinkmann, T. Becker, F. Zimmermann, C. Kreuzel, T. Gahlmann, M. Theisen, T. Haeger, S. Olthof, C. Tückmantel, M. Günster, *Nature* **604** No 7905, 280 (2022).
2. Y. Ding, B. Ding, H. Kanda, O.J. Usiobo, T. Gallet, Z. Yang, Y. Liu, H. Huang, J. Sheng, C. Liu, *Nat. Nanotechnol.* **17**, 598 (2022).
3. R. York, S.E. Bell, *Energy Res. Social Sci.* **51**, 40 (2019).
4. A.J. Chapman, B.C. McLellan, T. Tezuka, *Appl. Energy* **219**, 187 (2018).
5. K.A.S. Singh, M.K. Mohammed, A.E. Shalan, *Solar Energy* **223**, 193 (2021).
6. A.K. Al-Mousoi, M. Mehde, A.M. Al-Gebori, *IOP Conf. Ser.: Mater. Sci. Eng.* **757**, 012039 (2020).

7. M.K. Mohammed, A.K. Al-Mousoi, *Optik* **127** No 20, 9848 (2016).
8. J.P. Correa-Baena, M. Saliba, T. Buonassisi, M. Grätzel, A. Abate, W. Tress, A.J.S. Hagfeldt, *Science* **358** No 6364, 739 (2017).
9. M.D. Humadi, H.T. Hussein, M.S. Mohamed, M.K. Mohammed, E. Kayahan, *Opt. Mater.* **112**, 110794 (2021).
10. M.J. Kadhim, M.K. Mohammed, *Mater. Res. Bull.* **158**, 112047 (2022).
11. M.K. Mohammed, A.K. Al-Mousoi, S.M. Majeed, S. Singh, A. Kumar, R. Pandey, J. Madan, D.S. Ahmed, D. Dastan, *Energy Fuel*. **36** No 21, 13187 (2022).
12. S.H. Kareem, M.H. Elewi, A.M. Naji, D.S. Ahmed, M.K. Mohammed, *Chem. Eng. J.* **443**, 136469 (2022).
13. M.K. Mohammed, M.S. Jabir, H.G. Abdulzahraa, S.H. Mohammed, W.K. Al-Azzawi, D.S. Ahmed, S. Singh, A. Kumar, S. Asaithambi, M. Shekargoar, *RSC Adv.* **12** No 32, 20461 (2022).
14. M.M. Moharam, A.N. El Shazly, K.V. Anand, D.E. Rayan, M.K. Mohammed, M.M. Rashad, A.E. Shalan, *Top. Curr. Chem.* **379** No 3, 1 (2021).
15. A.K. Al-Mousoi, M.K. Mohammed, *J. Sol-Gel Sci. Technol.* **96** No 3, 659 (2020).

## Проектування та аналіз властивостей наноструктур MASnL<sub>3</sub>, легованих Cu<sub>2</sub>O

Ankit Mishra<sup>1</sup>, Manoj Kumar Nigam<sup>2</sup>

<sup>1</sup> Department of Electrical Engineering, MATS University, Raipur, India

<sup>2</sup> Department of Electrical Engineering, MATS University, Raipur, India

У статті ми моделюємо йодид метиламонію олова MASnL<sub>3</sub> з оксидом цинку-алюмінію nZnO-Al, легованим Cu<sub>2</sub>O. Ця базова структура демонструє обнадійливі результати порівняно з попередніми даними. Ми використовуємо інструмент високого моделювання SCAPS-1D для дослідження ВАХ, адмітансу, ширини забороненої зони та щільності струму базової структури FTO/Cu<sub>2</sub>O/MASnL<sub>3</sub>/nZnO-Al. У цьому дослідженні було досягнуто позитивних результатів і PCE 24,2 %. Тут необхідна анодна композиція з таким високим потенціалом роботи, щоб пристрій працював більш ефективно. Нова безсвинцева фотоелектрична матриця на основі перовскіту на основі сонячної батареї MASnL<sub>3</sub> із різними параметрами (SCAPS-1D) була створена та змодельована за допомогою моделювання одновимірної фотоелектричної сонячної емності. Результати показали, що товщина шару поглинача може мати значний вплив на PCE пристрою, і було визначено, що 250 нм є ідеальною товщиною для шару поглинача. У цих дослідженнях ми ввели дві різні щільності дефектів на кожному шарі PEC, щоб створити стандартне середовище, і результати є багатобічними. Використовувались різні провідні матеріали та шари, включаючи шари електродів, ETL та HTL. При температурі 300 К PEC працює ефективно. Також спостерігається, що зміна температури може знизити загальну ефективність пристрою.

**Ключові слова:** MASnL<sub>3</sub>, nZnO-Al, Наноструктури, Перовскіт, SCAPS-1D, Обчислювальне моделювання.